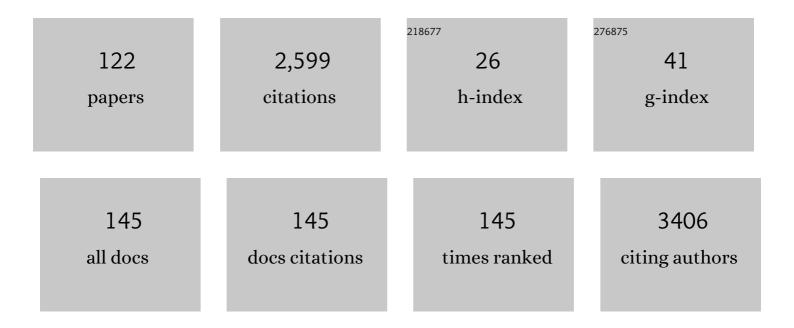
List of Publications by Year in descending order

Source: https://exaly.com/author-pdf/2811376/publications.pdf Version: 2024-02-01



SHI-TING FENC

#	Article	IF	CITATIONS
1	Optimization of the tumour response threshold in advanced gastroenteropancreatic neuroendocrine carcinomas treated with cisplatin/etoposide combined chemotherapy. European Journal of Radiology, 2022, 147, 110119.	2.6	0
2	Utility of Quantitative Metrics From Dual-Layer Spectral-Detector CT for Differentiation of Pancreatic Neuroendocrine Tumor and Neuroendocrine Carcinoma. American Journal of Roentgenology, 2022, 218, 999-1009.	2.2	7
3	Neoadjuvant programmed cell death 1 blockade combined with chemotherapy for resectable esophageal squamous cell carcinoma. , 2022, 10, e003497.		82
4	Discrepancies between Nonalcoholic and Metabolic-associated Fatty Liver Disease by Multiple Steatosis Assessment. Journal of Clinical and Translational Hepatology, 2022, 000, 000-000.	1.4	3
5	Noninvasive Imaging Evaluation Based on Computed Tomography of the Efficacy of Initial Transarterial Chemoembolization to Predict Outcome in Patients with Hepatocellular Carcinoma. Journal of Hepatocellular Carcinoma, 2022, Volume 9, 273-288.	3.7	5
6	Deep Segmentation Feature-Based Radiomics Improves Recurrence Prediction of Hepatocellular Carcinoma. BME Frontiers, 2022, 2022, .	4.5	3
7	Lipid-Lowering Responses to Dyslipidemia Determine the Efficacy on Liver Enzymes in Metabolic Dysfunction-Associated Fatty Liver Disease with Hepatic Injuries: A Prospective Cohort Study. Diabetes, Metabolic Syndrome and Obesity: Targets and Therapy, 2022, Volume 15, 1173-1184.	2.4	5
8	Tumor fibrosis correlates with the survival of patients with pancreatic adenocarcinoma and is predictable using clinicoradiological features. European Radiology, 2022, 32, 6314-6326.	4.5	3
9	The role of neoadjuvant conventional transarterial chemoembolization with radiofrequency ablation in the treatment of recurrent hepatocellular carcinoma after initial hepatectomy with microvascular invasion. International Journal of Hyperthermia, 2022, 39, 688-696.	2.5	2
10	Vitamin D Status Presents Different Relationships with Severity in Metabolic-Associated Fatty Liver Disease Patients with or without Hepatitis B Infection. Nutrients, 2022, 14, 2114.	4.1	4
11	Intestinal fibrosis classification in patients with Crohn's disease using CT enterography–based deep learning: comparisons with radiomics and radiologists. European Radiology, 2022, 32, 8692-8705.	4.5	30
12	Deep Semantic Segmentation Feature-Based Radiomics for the Classification Tasks in Medical Image Analysis. IEEE Journal of Biomedical and Health Informatics, 2021, 25, 2655-2664.	6.3	20
13	A novel identification system combining diffusion kurtosis imaging with conventional magnetic resonance imaging to assess intestinal strictures in patients with Crohn's disease. Abdominal Radiology, 2021, 46, 936-947.	2.1	10
14	Longitudinal radiomics algorithm of posttreatment computed tomography images for early detecting recurrence of hepatocellular carcinoma after resection or ablation. Translational Oncology, 2021, 14, 100866.	3.7	11
15	Quantification of brown adipose tissue in vivo using synthetic magnetic resonance imaging: an experimental study with mice model. Quantitative Imaging in Medicine and Surgery, 2021, 12, 0-0.	2.0	3
16	Degree of Creeping Fat Assessed by Computed Tomography Enterography is Associated with Intestinal Fibrotic Stricture in Patients with Crohn's Disease: A Potentially Novel Mesenteric Creeping Fat Index. Journal of Crohn's and Colitis, 2021, 15, 1161-1173.	1.3	45
17	A Pre-Operative Prognostic Score for Patients With Advanced Hepatocellular Carcinoma Who Underwent Resection. Frontiers in Oncology, 2021, 11, 569515.	2.8	1
18	Lack of Response to Transarterial Chemoembolization for Intermediate-Stage Hepatocellular Carcinoma: Abandon or Repeat?. Radiology, 2021, 298, 680-692.	7.3	23

#	Article	IF	CITATIONS
19	The Chinese guidelines for the diagnosis and treatment of pancreatic neuroendocrine neoplasms (2020). Journal of Pancreatology, 2021, 4, 1-17.	0.9	4
20	Microvascular Invasion Status and Its Survival Impact in Hepatocellular Carcinoma Depend on Tissue Sampling Protocol. Annals of Surgical Oncology, 2021, 28, 6747-6757.	1.5	11
21	Hepatic mosaic enhancement pattern correlates with increased inflammatory activity and adverse therapeutic outcomes in patients with Crohn's disease. Abdominal Radiology, 2021, 46, 3149-3158.	2.1	0
22	Apolipoproteins and liver parameters optimize cardiovascular disease risk-stratification in nonalcoholic fatty liver disease. Digestive and Liver Disease, 2021, 53, 1610-1619.	0.9	8
23	Nomogram development and validation to predict hepatocellular carcinoma tumor behavior by preoperative gadoxetic acid-enhanced MRI. European Radiology, 2021, 31, 8615-8627.	4.5	21
24	A computed tomography (CT)-derived radiomics approach for predicting primary co-mutations involving TP53 and epidermal growth factor receptor (EGFR) in patients with advanced lung adenocarcinomas (LUAD). Annals of Translational Medicine, 2021, 9, 545-545.	1.7	6
25	Normalization of γ-glutamyl transferase levels is associated with better metabolic control in individuals with nonalcoholic fatty liver disease. BMC Gastroenterology, 2021, 21, 215.	2.0	9
26	Considerable effects of imaging sequences, feature extraction, feature selection, and classifiers on radiomics-based prediction of microvascular invasion in hepatocellular carcinoma using magnetic resonance imaging. Quantitative Imaging in Medicine and Surgery, 2021, 11, 1836-1853.	2.0	24
27	Distinct Dose-Dependent Association of Free Fatty Acids with Diabetes Development in Nonalcoholic Fatty Liver Disease Patients. Diabetes and Metabolism Journal, 2021, 45, 417-429.	4.7	7
28	3D DenseNet Deep Learning Based Preoperative Computed Tomography for Detecting Myasthenia Gravis in Patients With Thymoma. Frontiers in Oncology, 2021, 11, 631964.	2.8	8
29	Predicting the recurrence risk of pancreatic neuroendocrine neoplasms after radical resection using deep learning radiomics with preoperative computed tomography images. Annals of Translational Medicine, 2021, 9, 833-833.	1.7	14
30	Development and Validation of a Novel Computed-Tomography Enterography Radiomic Approach for Characterization of Intestinal Fibrosis in Crohn's Disease. Gastroenterology, 2021, 160, 2303-2316.e11.	1.3	57
31	A narrative review of multiple endocrine neoplasia syndromes: genetics, clinical features, imaging findings, and diagnosis. Annals of Translational Medicine, 2021, 9, 944-944.	1.7	5
32	Preoperative Prediction of Cytokeratin 19 Expression for Hepatocellular Carcinoma with Deep Learning Radiomics Based on Gadoxetic Acid-Enhanced Magnetic Resonance Imaging. Journal of Hepatocellular Carcinoma, 2021, Volume 8, 795-808.	3.7	12
33	Native T1 Mapping and Magnetization Transfer Imaging in Grading Bowel Fibrosis in Crohn's Disease: A Comparative Animal Study. Biosensors, 2021, 11, 302.	4.7	9
34	Computed Tomography-Based Radiomics Nomogram: Potential to Predict Local Recurrence of Gastric Cancer After Radical Resection. Frontiers in Oncology, 2021, 11, 638362.	2.8	6
35	Accurate and Feasible Deep Learning Based Semi-Automatic Segmentation in CT for Radiomics Analysis in Pancreatic Neuroendocrine Neoplasms. IEEE Journal of Biomedical and Health Informatics, 2021, 25, 3498-3506.	6.3	17
36	Regional liver function analysis with gadoxetic acid–enhanced MRI and virtual hepatectomy: prediction of postoperative short-term outcomes for HCC. European Radiology, 2021, 31, 4720-4730.	4.5	15

#	Article	IF	CITATIONS
37	Neoadjuvant PD-1 blockade in combination with chemotherapy for patients with resectable esophageal squamous cell carcinoma Journal of Clinical Oncology, 2021, 39, 220-220.	1.6	7
38	Steatosis grading consistency between controlled attenuation parameter and MRI-PDFF in monitoring metabolic associated fatty liver disease. Therapeutic Advances in Chronic Disease, 2021, 12, 204062232110331.	2.5	19
39	Predicting response to immunotherapy plus chemotherapy in patients with esophageal squamous cell carcinoma using non-invasive Radiomic biomarkers. BMC Cancer, 2021, 21, 1167.	2.6	12
40	A Type I Collagen-Targeted MR Imaging Probe for Staging Fibrosis in Crohn's Disease. Frontiers in Molecular Biosciences, 2021, 8, 762355.	3.5	8
41	Prediction of Early Treatment Response to Initial Conventional Transarterial Chemoembolization Therapy for Hepatocellular Carcinoma by Machine-Learning Model Based on Computed Tomography. Journal of Hepatocellular Carcinoma, 2021, Volume 8, 1473-1484.	3.7	9
42	Varied Relationship of Lipid and Lipoprotein Profiles to Liver Fat Content in Phenotypes of Metabolic Associated Fatty Liver Disease. Frontiers in Endocrinology, 2021, 12, 691556.	3.5	7
43	P-L11 Comparison of clinical efficacy between LAPS and ALPPS in the Treatment of Hepatitis B Virus-related Hepatocellular Carcinoma. British Journal of Surgery, 2021, 108, .	0.3	Ο
44	Magnetisation transfer imaging adds information to conventional MRIs to differentiate inflammatory from fibrotic components of small intestinal strictures in Crohn's disease. European Radiology, 2020, 30, 1938-1947.	4.5	21
45	Early Predictors of Cardiovascular Disease Risk in Nonalcoholic Fatty Liver Disease: Non-obese Versus Obese Patients. Digestive Diseases and Sciences, 2020, 65, 1850-1860.	2.3	19
46	Preoperative Prediction of Pancreatic Neuroendocrine Neoplasms Grading Based on Enhanced Computed Tomography Imaging: Validation of Deep Learning with a Convolutional Neural Network. Neuroendocrinology, 2020, 110, 338-350.	2.5	43
47	A CT-derived deep neural network predicts for programmed death ligand-1 expression status in advanced lung adenocarcinomas. Annals of Translational Medicine, 2020, 8, 930-930.	1.7	13
48	<p>Diameter of Superior Rectal Vein – CT Predictor of KRAS Mutation in Rectal Carcinoma</p> . Cancer Management and Research, 2020, Volume 12, 10919-10928.	1.9	7
49	<a a="" case="" cava="" evaluation="" huge="" inferior="" leiomyosarcoma:="" of="" precise="" preoperative="" vena="" with<br="">Gadobutrol-Enhanced MRI. Cancer Management and Research, 2020, Volume 12, 7929-7939.	1.9	8
50	Hepatic nodules with arterial phase hyperenhancement and washout on enhanced computed tomography/magnetic resonance imaging: how to avoid pitfalls. Abdominal Radiology, 2020, 45, 3730-3742.	2.1	6
51	CT-based radiomics for preoperative prediction of early recurrent hepatocellular carcinoma: technical reproducibility of acquisition and scanners. Radiologia Medica, 2020, 125, 697-705.	7.7	63
52	Precise fibrosis staging with shear wave elastography in chronic hepatitis B depends on liver inflammation and steatosis. Hepatology International, 2020, 14, 190-201.	4.2	19
53	Hepatocellular carcinoma with hilar bile duct tumor thrombus versus hilar Cholangiocarcinoma on enhanced computed tomography: a diagnostic challenge. BMC Cancer, 2020, 20, 54.	2.6	13
54	Clinical and CT imaging features of 2019 novel coronavirus disease (COVID-19). Journal of Infection, 2020, 81, 147-178.	3.3	53

#	Article	IF	CITATIONS
55	Hepatic resection versus transarterial chemoembolization in infiltrative hepatocellular carcinoma: A multicenter study. Journal of Gastroenterology and Hepatology (Australia), 2020, 35, 2220-2228.	2.8	4
56	Feasibility of multi-parametric magnetic resonance imaging combined with machine learning in the assessment of necrosis of osteosarcoma after neoadjuvant chemotherapy: a preliminary study. BMC Cancer, 2020, 20, 322.	2.6	19
57	CT-based radiomics scores predict response to neoadjuvant chemotherapy and survival in patients with gastric cancer. BMC Cancer, 2020, 20, 468.	2.6	40
58	Comparison of Three Magnetization Transfer Ratio Parameters for Assessment of Intestinal Fibrosis in Patients with Crohn's Disease. Korean Journal of Radiology, 2020, 21, 290.	3.4	11
59	Multifunctionalized Microscale Ultrasound Contrast Agents for Precise Theranostics of Malignant Tumors. Contrast Media and Molecular Imaging, 2019, 2019, 1-18.	0.8	10
60	Diffusion Kurtosis MR Imaging versus Conventional Diffusion-Weighted Imaging for Distinguishing Hepatocellular Carcinoma from Benign Hepatic Nodules. Contrast Media and Molecular Imaging, 2019, 2019, 1-10.	0.8	4
61	Prediction of type 2 diabetes mellitus using noninvasive MRI quantitation of visceral abdominal adiposity tissue volume. Quantitative Imaging in Medicine and Surgery, 2019, 9, 1076-1086.	2.0	10
62	Pancreatic tumor in type 1 autoimmune pancreatitis: a diagnostic challenge. BMC Cancer, 2019, 19, 814.	2.6	12
63	Effect of orlistat on liver fat content in patients with nonalcoholic fatty liver disease with obesity: assessment using magnetic resonance imaging-derived proton density fat fraction. Therapeutic Advances in Gastroenterology, 2019, 12, 175628481987904.	3.2	30
64	Constructing an experiential education model in undergraduate radiology education by the utilization of the picture archiving and communication system (PACS). BMC Medical Education, 2019, 19, 383.	2.4	10
65	Preoperative prediction of microvascular invasion in hepatocellular cancer: a radiomics model using Gd-EOB-DTPA-enhanced MRI. European Radiology, 2019, 29, 4648-4659.	4.5	144
66	Pretreatment prediction of immunoscore in hepatocellular cancer: a radiomics-based clinical model based on Gd-EOB-DTPA-enhanced MRI imaging. European Radiology, 2019, 29, 4177-4187.	4.5	110
67	Insulin resistance exhibits varied metabolic abnormalities in nonalcoholic fatty liver disease, chronic hepatitis B and the combination of the two: a cross-sectional study. Diabetology and Metabolic Syndrome, 2019, 11, 45.	2.7	9
68	Microvascular Invasion as a Predictor of Response to Treatment with Sorafenib and Transarterial Chemoembolization for Recurrent Intermediate-Stage Hepatocellular Carcinoma. Radiology, 2019, 292, 237-247.	7.3	53
69	Imaging biomarkers for well and moderate hepatocellular carcinoma: preoperative magnetic resonance image and histopathological correlation. BMC Cancer, 2019, 19, 364.	2.6	15
70	MRI T2-Weighted Imaging and Fat-Suppressed T2-Weighted Imaging Image Fusion Technology Improves Image Discriminability for the Evaluation of Anal Fistulas. Korean Journal of Radiology, 2019, 20, 429.	3.4	12
71	CT-based peritumoral radiomics signatures to predict early recurrence in hepatocellular carcinoma after curative tumor resection or ablation. Cancer Imaging, 2019, 19, 11.	2.8	120
72	Different predictors of steatosis and fibrosis severity among lean, overweight and obese patients with nonalcoholic fatty liver disease. Digestive and Liver Disease, 2019, 51, 1392-1399.	0.9	25

#	Article	IF	CITATIONS
73	A novel collagen area fraction index to quantitatively assess bowel fibrosis in patients with Crohn's disease. BMC Gastroenterology, 2019, 19, 180.	2.0	5
74	IVIM with fractional perfusion as a novel biomarker for detecting and grading intestinal fibrosis in Crohn's disease. European Radiology, 2019, 29, 3069-3078.	4.5	26
75	Ability of DWI to characterize bowel fibrosis depends on the degree of bowel inflammation. European Radiology, 2019, 29, 2465-2473.	4.5	13
76	Prediction of sorafenib treatment–related gene expression for hepatocellular carcinoma: preoperative MRI and histopathological correlation. European Radiology, 2019, 29, 2272-2282.	4.5	14
77	Computed Tomography and Magnetic Resonance Imaging-aided Diagnosis of Primary Essential Cutis Verticis Gyrata: A Case Report with 5-year Follow-up and Review of the Literature. Current Medical Imaging, 2019, 15, 906-910.	0.8	3
78	T2* Mapping to characterize intestinal fibrosis in crohn's disease. Journal of Magnetic Resonance Imaging, 2018, 48, 829-836.	3.4	13
79	Characterization of Degree of Intestinal Fibrosis in Patients with Crohn Disease by Using Magnetization Transfer MR Imaging. Radiology, 2018, 287, 494-503.	7.3	81
80	IDDF2018-ABS-0098â€Preoperative prediction of microvascular invasion in hepatocellular cancer: a radiomics model using GD-EOB-DTPA enhanced MRI. , 2018, , .		1
81	CT Enterography score: a potential predictor for severity assessment of active ulcerative colitis. BMC Gastroenterology, 2018, 18, 173.	2.0	11
82	Tumor Segmentation in Contrast-Enhanced Magnetic Resonance Imaging for Nasopharyngeal Carcinoma: Deep Learning with Convolutional Neural Network. BioMed Research International, 2018, 2018, 1-7.	1.9	41
83	Combined Volumetric and Density Analyses of Contrast-Enhanced CT Imaging to Assess Drug Therapy Response in Gastroenteropancreatic Neuroendocrine Diffuse Liver Metastasis. Contrast Media and Molecular Imaging, 2018, 2018, 1-10.	0.8	3
84	Fully Automated Delineation of Gross Tumor Volume for Head and Neck Cancer on PET-CT Using Deep Learning: A Dual-Center Study. Contrast Media and Molecular Imaging, 2018, 2018, 1-12.	0.8	71
85	Prediction of Microvascular Invasion in Hepatocellular Carcinoma: Preoperative Gd-EOB-DTPA-Dynamic Enhanced MRI and Histopathological Correlation. Contrast Media and Molecular Imaging, 2018, 2018, 1-9.	0.8	50
86	Non-enhanced Pattern on Contrast-Enhanced Ultrasound in the Local Efficacy Assessment of Irreversible Electroporation Ablation of Pancreatic Adenocarcinoma. Ultrasound in Medicine and Biology, 2018, 44, 1986-1995.	1.5	1
87	CT evaluation of response in advanced gastroenteropancreatic neuroendocrine tumors treated with long-acting-repeatable octreotide: what is the optimal size variation threshold?. European Radiology, 2018, 28, 5250-5257.	4.5	3
88	Diffusion kurtosis MRI versus conventional diffusionâ€weighted imaging for evaluating inflammatory activity in Crohn's disease. Journal of Magnetic Resonance Imaging, 2018, 47, 702-709.	3.4	14
89	Nano-sized Ultrasound Contrast Agents for Cancer Therapy and Theranostics. Current Pharmaceutical Design, 2018, 23, 5403-5412.	1.9	5
90	Early evaluation of sunitinib for the treatment of advanced gastroenteropancreatic neuroendocrine neoplasms via CT imaging: RECIST 1.1 or Choi Criteria?. BMC Cancer, 2017, 17, 154.	2.6	30

#	Article	IF	CITATIONS
91	Somatostatin receptor expression indicates improved prognosis in gastroenteropancreatic neuroendocrine neoplasm, and octreotide long-acting release is effective and safe in Chinese patients with advanced gastroenteropancreatic neuroendocrine tumors. Oncology Letters, 2017, 13, 1165-1174.	1.8	52
92	Diffusion-weighted MRI Enables to Accurately Grade Inflammatory Activity in Patients of Ileocolonic Crohn's Disease. Inflammatory Bowel Diseases, 2017, 23, 244-253.	1.9	38
93	Differentiation between gastrointestinal schwannomas and gastrointestinal stromal tumors by computed tomography. Oncology Letters, 2017, 13, 3746-3752.	1.8	13
94	Dualâ€responsive crosslinked micelles of a multifunctional graft copolymer for drug delivery applications. Journal of Polymer Science Part A, 2017, 55, 1536-1546.	2.3	5
95	Sunitinib is effective and tolerable in Chinese patients with advanced pancreatic neuroendocrine tumors: a multicenter retrospective study in China. Cancer Chemotherapy and Pharmacology, 2017, 80, 507-516.	2.3	12
96	The role of elevated serum procalcitonin in neuroendocrine neoplasms of digestive system. Clinical Biochemistry, 2017, 50, 982-987.	1.9	17
97	An Individually Optimized Protocol of Contrast Medium Injection in Enhanced CT Scan for Liver Imaging. Contrast Media and Molecular Imaging, 2017, 2017, 1-8.	0.8	12
98	Pancreatic schwannoma: a case report and an updated 40-year review of the literature yielding 68 cases. BMC Cancer, 2017, 17, 853.	2.6	30
99	Quantitative evaluation of Gd-EOB-DTPA uptake in focal liver lesions by using T1 mapping: differences between hepatocellular carcinoma, hepatic focal nodular hyperplasia and cavernous hemangioma. Oncotarget, 2017, 8, 65435-65444.	1.8	16
100	Gadolinium/DOTA functionalized poly(ethylene glycol)-block-poly(acrylamide-co-acrylonitrile) micelles with synergistically enhanced cellular uptake for cancer theranostics. RSC Advances, 2016, 6, 50534-50542.	3.6	19
101	Surgical management for non-functional pancreatic neuroendocrine neoplasms with synchronous liver metastasis: A consensus from the Chinese Study Group for Neuroendocrine Tumors (CSNET). International Journal of Oncology, 2016, 49, 1991-2000.	3.3	27
102	Gd-EOB-DTPA-enhanced magnetic resonance imaging combined with T1 mapping predicts the degree of differentiation in hepatocellular carcinoma. BMC Cancer, 2016, 16, 625.	2.6	30
103	Nanoparticles for Colorectal Cancer Targeted Drug Delivery and MR Imaging: Current Situation and Perspectives. Current Cancer Drug Targets, 2016, 16, 536-550.	1.6	11
104	Ultrasound virtual endoscopy: Polyp detection and reliability of measurement in an <i>in vitro</i> study with pig intestine specimens. World Journal of Gastroenterology, 2016, 22, 3355-3362.	3.3	1
105	Evaluation of intestinal tuberculosis by multi-slice computed tomography enterography. BMC Infectious Diseases, 2015, 15, 577.	2.9	16
106	Selfâ€assembled UCSTâ€Type Micelles as Potential Drug Carriers for Cancer Therapeutics. Macromolecular Chemistry and Physics, 2015, 216, 1014-1023.	2.2	53
107	Cholangiocarcinoma: spectrum of appearances on Gd-EOB-DTPA-enhanced MR imaging and the effect of biliary function on signal intensity. BMC Cancer, 2015, 15, 38.	2.6	14
108	Spectrum of appearances on CT and MRI of hepatic epithelioid hemangioendothelioma. BMC Gastroenterology, 2015, 15, 69.	2.0	41

#	Article	IF	CITATIONS
109	pH-Sensitive Nanomicelles for Controlled and Efficient Drug Delivery to Human Colorectal Carcinoma LoVo Cells. PLoS ONE, 2014, 9, e100732.	2.5	43
110	MR Quantification of Total Liver Fat in Patients with Impaired Glucose Tolerance and Healthy Subjects. PLoS ONE, 2014, 9, e111283.	2.5	29
111	CT Findings of Intrarenal Yolk Sac Tumor with Tumor Thrombus Extending into the Inferior Vena Cava: A Case Report. Korean Journal of Radiology, 2014, 15, 641.	3.4	9
112	Pancreatic neuroendocrine tumours: correlation between MSCT features and pathological classification. European Radiology, 2014, 24, 2945-2952.	4.5	41
113	Diagnostic and post-treatment CT appearance of biopsy proven mixed cryptococcus and candida cholangitis. Journal of X-Ray Science and Technology, 2014, 22, 727-733.	1.0	3
114	Functional magnetic resonance cholangiography enhanced with Gd-EOB-DTPA: Effect of liver function on biliary system visualization. Journal of Magnetic Resonance Imaging, 2014, 39, 1254-1258.	3.4	6
115	CT Evaluation of Gastroenteric Neuroendocrine Tumors: Relationship Between CT Features and the Pathologic Classification. American Journal of Roentgenology, 2014, 203, W260-W266.	2.2	6
116	The influence of upper limb position on the effect of a contrast agent in chest CT enhancement. European Journal of Radiology, 2013, 82, 1023-1027.	2.6	2
117	CT Enterography in Evaluating Postoperative Recurrence of Crohn's Disease after Ileocolic Resection. Inflammatory Bowel Diseases, 2013, 19, 977-982.	1.9	45
118	Image-Derived Arterial Input Function in Dynamic Positron Emission Tomography–Computed Tomography. Journal of Computer Assisted Tomography, 2012, 36, 762-767.	0.9	7
119	Evaluation of angiogenesis in colorectal carcinoma with multidetector-row CT multislice perfusion imaging. European Journal of Radiology, 2010, 75, 191-196.	2.6	18
120	Multiphasic MDCT in small bowel volvulus. European Journal of Radiology, 2010, 76, e13-e18.	2.6	24
121	Radiation dose and cancer risk from pediatric CT examinations on 64-slice CT: A phantom study. European Journal of Radiology, 2010, 76, e19-e23.	2.6	70
122	CT and MR imaging characteristics of infantile hepatic hemangioendothelioma. European Journal of Radiology, 2010, 76, e24-e29.	2.6	23